

AD

TECHNICAL REPORT ARCCB-TR-99021

**COATING EVALUATION USING ANALYTICAL
AND EXPERIMENTAL DISPERSION CURVES**

**B. KNIGHT
M. HUSSAIN
J. FRANKEL**

**J. F. COX
J. BRAUNSTEIN
P. J. COTE**

A. ABBATE

NOVEMBER 1999



**US ARMY ARMAMENT RESEARCH,
DEVELOPMENT AND ENGINEERING CENTER
CLOSE COMBAT ARMAMENTS CENTER
BENÉT LABORATORIES
WATERVLIET, N.Y. 12189-4050**



APPROVED FOR PUBLIC RELEASE; DISTRIBUTION UNLIMITED

DTIC QUALITY INSPECTED 2

19991213 017

DISCLAIMER

The findings in this report are not to be construed as an official Department of the Army position unless so designated by other authorized documents.

The use of trade name(s) and/or manufacturer(s) does not constitute an official endorsement or approval.

DESTRUCTION NOTICE

For classified documents, follow the procedures in DoD 5200.22-M, Industrial Security Manual, Section II-19, or DoD 5200.1-R, Information Security Program Regulation, Chapter IX.

For unclassified, limited documents, destroy by any method that will prevent disclosure of contents or reconstruction of the document.

For unclassified, unlimited documents, destroy when the report is no longer needed. Do not return it to the originator.

REPORT DOCUMENTATION PAGE

Form Approved
OMB No. 0704-0188

Public reporting burden for this collection of information is estimated to average 1 hour per response, including the time for reviewing instructions, searching existing data sources, gathering and maintaining the data needed, and completing and reviewing the collection of information. Send comments regarding this burden estimate or any other aspect of this collection of information, including suggestions for reducing this burden, to Washington Headquarters Services, Directorate for Information Operations and Reports, 1215 Jefferson Davis Highway, Suite 1204, Arlington, VA 22202-4302, and to the Office of Management and Budget, Paperwork Reduction Project (0704-0188), Washington, DC 20503.

1. AGENCY USE ONLY (Leave blank)	2. REPORT DATE	3. REPORT TYPE AND DATES COVERED	
	November 1999	Final	
4. TITLE AND SUBTITLE COATING EVALUATION USING ANALYTICAL AND EXPERIMENTAL DISPERSION CURVES			5. FUNDING NUMBERS PRON No. 8LRMFARD77
6. AUTHOR(S) B. Knight, M. Hussain, J. Frankel, J.F. Cox, J. Braunstein, P.J. Cote, and A. Abbate (Textron Systems, Wilmington, MA)			
7. PERFORMING ORGANIZATION NAME(S) AND ADDRESS(ES) U.S. Army ARDEC Benet Laboratories, AMSTA-AR-CCB-O Watervliet, NY 12189-4050		8. PERFORMING ORGANIZATION REPORT NUMBER ARCCB-TR-99021	
9. SPONSORING / MONITORING AGENCY NAME(S) AND ADDRESS(ES) U.S. Army ARDEC Close Combat Armaments Center Picatinny Arsenal, NJ 07806-5000		10. SPONSORING / MONITORING AGENCY REPORT NUMBER	
11. SUPPLEMENTARY NOTES Presented at the 26 th Annual Review of Progress in Quantitative Nondestructive Evaluation, Montreal, Canada, 25-31 July 1999. Published in <i>Review of Progress in Quantitative Nondestructive Evaluation</i> .			
12a. DISTRIBUTION / AVAILABILITY STATEMENT Approved for public release; distribution unlimited.		12b. DISTRIBUTION CODE	
13. ABSTRACT (Maximum 200 words) Well-bonded or "welded" contact and poorly bonded or "smooth" contact bonds were studied. As examples of welded contact bonds, we used sputtered tantalum and electrodeposited high contraction chromium coatings that were deposited onto steel substrates under controlled conditions. In order to simulate smooth contact coatings, thin sheets of nickel and tantalum were epoxied to copper and steel substrates, respectively. We used the method originated by Cielo et al. to gather data consisting of laser generation of the surface waves in an annular ring and laser detection in the center. Wavelet techniques were used on the surface wave-detected signals in order to obtain the experimental dispersion (velocity-frequency) curves. The experimental dispersion curves were compared to theoretical curves to give insight into the bond quality. It was found that the experimental results correlated well with the theory for the welded case.			
14. SUBJECT TERMS Coatings, Dispersion Curves, Welded Contact Bonds, Smooth Contact Bonds, Wavelet Techniques, Tantalum, Chromium			15. NUMBER OF PAGES 11
16. PRICE CODE			
17. SECURITY CLASSIFICATION OF REPORT UNCLASSIFIED	18. SECURITY CLASSIFICATION OF THIS PAGE UNCLASSIFIED	19. SECURITY CLASSIFICATION OF ABSTRACT UNCLASSIFIED	20. LIMITATION OF ABSTRACT II

TABLE OF CONTENTS

	<u>Page</u>
INTRODUCTION.....	1
THEORY.....	2
EXPERIMENT.....	5
Samples	5
Laser System	6
Data Collection and Analysis.....	6
DISCUSSION AND RESULTS	7
CONCLUSIONS.....	9
REFERENCES.....	10

TABLES

1. Experimental Sample Parameters.....	6
--	---

LIST OF ILLUSTRATIONS

1. Layer and half space.....	2
2. Surface waves of different frequencies traveling in a layered material	4
3. Theoretical dispersion curves calculated from experimental parameters for the coating acoustically stiffer (left) and less stiff than the substrate (right), welded contact (a) and smooth contact (b)	5
4. Waveforms from the laser-generated surface waves (left) and their corresponding dispersion curves (right).....	8

INTRODUCTION

The life of mechanical components depends greatly on their surface condition. Cracks and other surface imperfections propagate into the bulk of the material causing failure. Exposure to extreme temperatures, pressures, stress pulses, and corrosive liquids or gases can magnify these effects and further shorten the life of the part. Metallic coatings are applied to protect the surface against crack propagation and thus against wear and erosion.

The effectiveness of the coating depends on its mechanical properties, thickness, cohesion, and adhesion to the substrate. These properties can vary from coating to coating of the same material, with subtle changes in substrate preparation, surface finish, and coating deposition parameters. Therefore, practical methods, preferably nondestructive, are needed to be able to measure properties one can associate with the quality of these coatings. Ultrasonics has been used successfully for years as a means of nondestructive material testing and evaluation. However, traditional ultrasonics requires the probes to be in contact with the test surface. Surface waves generated by laser impulse provide a dynamic method for evaluation of thin metallic coatings, which cannot be evaluated by other ultrasonic techniques or by other technologies using tomography.

The use of laser ultrasonics as a testing tool provides several advantages over classical ultrasonic methods. Near-field effects and couplant problems associated with conventional ultrasonics are eliminated. Measurements can also be made at high temperatures. Parts with odd shapes or curved surfaces can potentially be evaluated without preparation of special equipment for testing. Using lasers also allows for both generation and detection of a wide band of frequencies, which is important, especially when characterizing thin coatings of less than 100 μm .

Our objective was to evaluate the ability of theory and experiment to distinguish between good and poor bonds. Achenbach and Epstein (ref 1) have analyzed two different bonds, one of which they call "welded," and the other, known as "smooth" contact. Their analysis was conducted in terms of the boundary conditions defined between the layer and the half space. They showed that the dispersion relation gives insight into the bond quality between a coating and a substrate.

Surface waves are nondispersive in homogenous isotropic materials, but become dispersive in materials with coatings. For a dispersive signal, the determination of the acoustic velocity in the coating is not as straightforward as in the case when the signal is nondispersive. Wavelet analysis was used here to obtain dispersion curves (ref 2), the velocity-frequency relationship. The dispersion of a surface wave traveling in a coated material depends on the relative Rayleigh velocities of the substrate and coating and on the type of bond. Wavelet analysis also provided information about the material properties of both the coating and the substrate materials.

We simulated and provided experimental data for four cases and compared the predicted and experimentally obtained dispersion curves. These were for smooth and welded contacts, with the coating being acoustically stiffer and less stiff than the substrate. For the welded bond, we used sputtered tantalum on steel in one case and chromium electrodeposited on steel for the other. To simulate the smooth contact bond, we epoxied thin sheets of tantalum and nickel on steel and copper substrates, respectively. We used the method originated by Cielo et al. (ref 3) to gather

data consisting of laser generation of the surface waves in an annular ring and laser detection in the center.

THEORY

Waves that propagate along the free surface of a semi-infinite solid travel as Rayleigh surface waves. Rayleigh waves in a system consisting of a layer and half space, having different elastic properties, propagate in an infinite number of modes. Achenbach and Epstein (ref 1) have provided a two-dimensional analysis with various boundary conditions for free waves in a system consisting of layer (coating) and half space (substrate). Figure 1 illustrates an example of a layer and half space. The figure shows the dispersion relation in two dimensions r and z . Our study looks at the axisymmetric case in the coordinate system r , z , and θ .

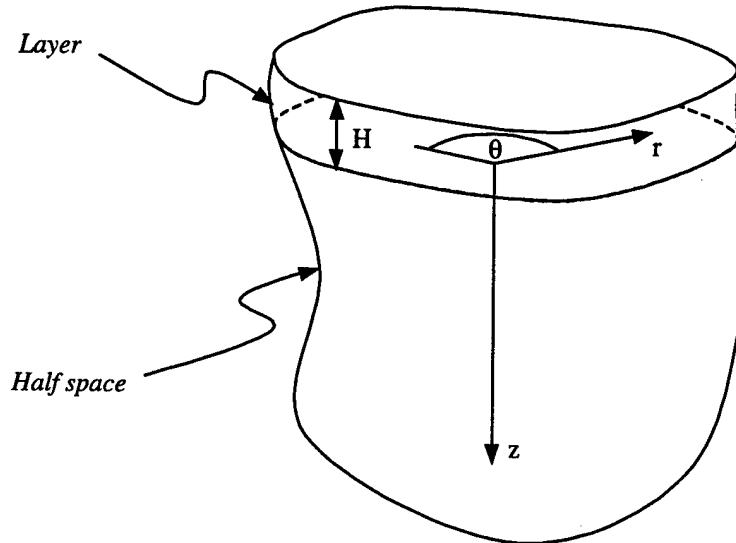


Figure 1. Layer and half space.

Using the Helmholtz decomposition (ref 4), we obtained the scalar and vector potential, and set up the required field quantities of elasticity, for the problem of a layer on an elastic half space in the axisymmetric case. The equation of equilibrium in terms of displacements can be written as

$$(\lambda + 2\mu) \nabla(\nabla \cdot \vec{u}) - \mu \nabla \times (\nabla \times \vec{u}) - \rho \frac{\partial^2 \vec{u}}{\partial t^2} = 0 \quad (1)$$

where λ , μ are the Lamé constants, ρ is the material density, and \vec{u} is the displacement. Using the Helmholtz decomposition (ref 4)

$$\vec{u} = \nabla \phi + \nabla \times \vec{\psi} \quad (2)$$

with

$$\nabla \cdot \vec{\psi} = 0 \quad (3)$$

The equation of motion can be reduced to the solutions of the following scalar and vector equations:

$$\nabla^2 \vec{\psi} - \frac{1}{V_s^2} \frac{\partial^2 \vec{\psi}}{\partial t^2} = 0 \quad \nabla^2 \phi - \frac{1}{V_l^2} \frac{\partial^2 \phi}{\partial t^2} = 0 \quad (4)$$

where

$$V_s^2 = \frac{\mu}{\rho} \quad V_l^2 = \frac{\lambda + 2\mu}{\rho} \quad (5)$$

Assuming the time factor of the form $e^{i\omega t}$, and c is the velocity of the wave, we define some parameters based on the elastic properties of the two elastic layers. The subscripts a and b reference the layer and half space, respectively.

$$q_a^2 = 1 - \frac{c^2}{V_{l_a}^2} \quad s_a^2 = 1 - \frac{c^2}{V_{s_a}^2} \quad k = \frac{\omega}{c} \quad (6)$$

Similar parameters are defined for the half space. The solution of equation (4) in the layer can be written as

$$\phi_a(r, z, \theta) = \{A_a J_0(kr) e^{-q_a kz} + L_a J_0(kr) e^{q_a kz}\} e^{i\omega t} \quad (7)$$

$$\vec{\psi}_a(r, z, \theta) = \left\{ \begin{aligned} & \left[B_a J_1(kr) e^{-s_a kz}, C_a J_1(kr) e^{-s_a kz}, \frac{B_a}{s_a} J_0(kr) e^{-s_a kz} \right] \\ & + \left[M_a J_1(kr) e^{s_a kz}, N_a J_1(kr) e^{s_a kz}, -\frac{M_a}{s_a} J_0(kr) e^{s_a kz} \right] \end{aligned} \right\} e^{i\omega t} \quad (8)$$

The solution of equation (4) in the half space is

$$\phi_b(r, z, \theta) = \{A_b J_0(kr) e^{-q_b kz}\} e^{i\omega t} \quad (9)$$

$$\vec{\psi}_b(r, z, \theta) = \left\{ \begin{aligned} & \left[B_b J_1(kr) e^{-s_b kz}, C_b J_1(kr) e^{-s_b kz}, \frac{B_b}{s_b} J_0(kr) e^{-s_b kz} \right] \end{aligned} \right\} e^{i\omega t} \quad (10)$$

Free waves are plane harmonic waves with real phase velocities and wave numbers. Here the free waves in the coating can interact (or couple) with the waves in the half space, as seen in Figure 2. For the welded contact, the high and low frequency ends of the ultrasonic pulse, the Rayleigh waves travel with velocities characteristic of the coating and substrate, respectively. In between these values, the coupling provides intermediate velocities between the coating velocity and the substrate velocity. This is not so for the smooth contact when Rayleigh waves propagate in the system of coating and substrate, with their particular velocity-frequency relation determined by the boundary conditions between coating and substrate. The analysis results in dispersion curves that are distinct, and characteristic of the boundary conditions.

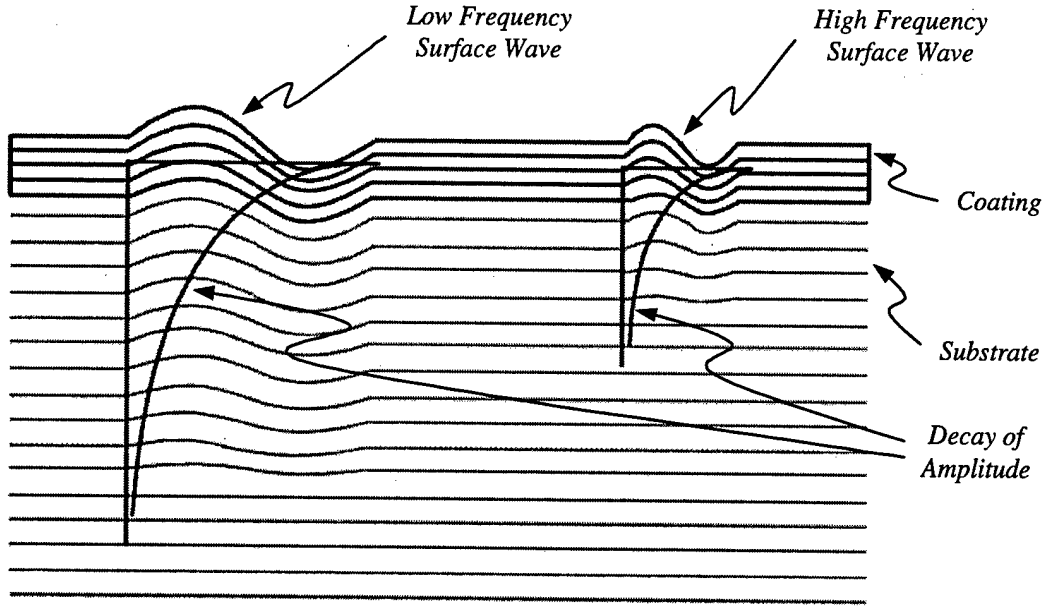


Figure 2. Surface waves of different frequencies traveling in a layered material.

The boundary conditions imposed characterize the bond between the layer and half space. Using boundary conditions analogous to Achenbach and Epstein (ref 1), we have obtained the dispersion relations for both cases.

The two bond conditions, welded and smooth contact, are described by the following boundary conditions. For welded contact, the boundary conditions are

$$\sigma_{z_a} = 0, \tau_{rz_a} = 0, \tau_{\theta z_a} = 0 \quad \text{at } z = -H \quad (11)$$

$$u_{z_a} = u_{z_b}, u_{r_a} = u_{r_b}, u_{\theta_a} = u_{\theta_b}, \tau_{rz_a} = \tau_{rz_b}, \tau_{\theta z_a} = \tau_{\theta z_b}, \sigma_{z_a} = \sigma_{z_b} \quad \text{at } z = 0 \quad (12)$$

and the smooth contact boundary conditions are

$$\sigma_{z_a} = 0, \tau_{rz_a} = 0, \tau_{\theta z_a} = 0 \quad \text{at } z = -H \quad (13)$$

$$u_{z_a} = u_{z_b}, \tau_{rz_a} = 0, \tau_{rz_b} = 0, \tau_{\theta z_a} = 0, \tau_{\theta z_b} = 0, \sigma_{z_a} = \sigma_{z_b} \quad \text{at } z = 0 \quad (14)$$

These boundary conditions lead to a set of nine homogenous equations involving geometric parameters, elastic constants, frequency, and acoustic velocity. For the solution to exist, the 9×9 determinant has to vanish for a set of velocities in a frequency range leading to the dispersion relation for the given geometry and material properties. Further, in absence of torsional motion this determinant reduces to the ones given by Achenbach and Epstein (ref 1).

Dispersion curves have been obtained from analysis using the above formulation for the cases that have been experimentally studied. These are for a smooth and welded contact, with the coating being acoustically stiffer and less stiff than the substrate. The theoretical dispersion

curves are shown in Figures 3(a) and (b). The material properties used to generate these curves (acoustic velocities and coating thickness) were taken from values that well represent the materials being experimentally examined.

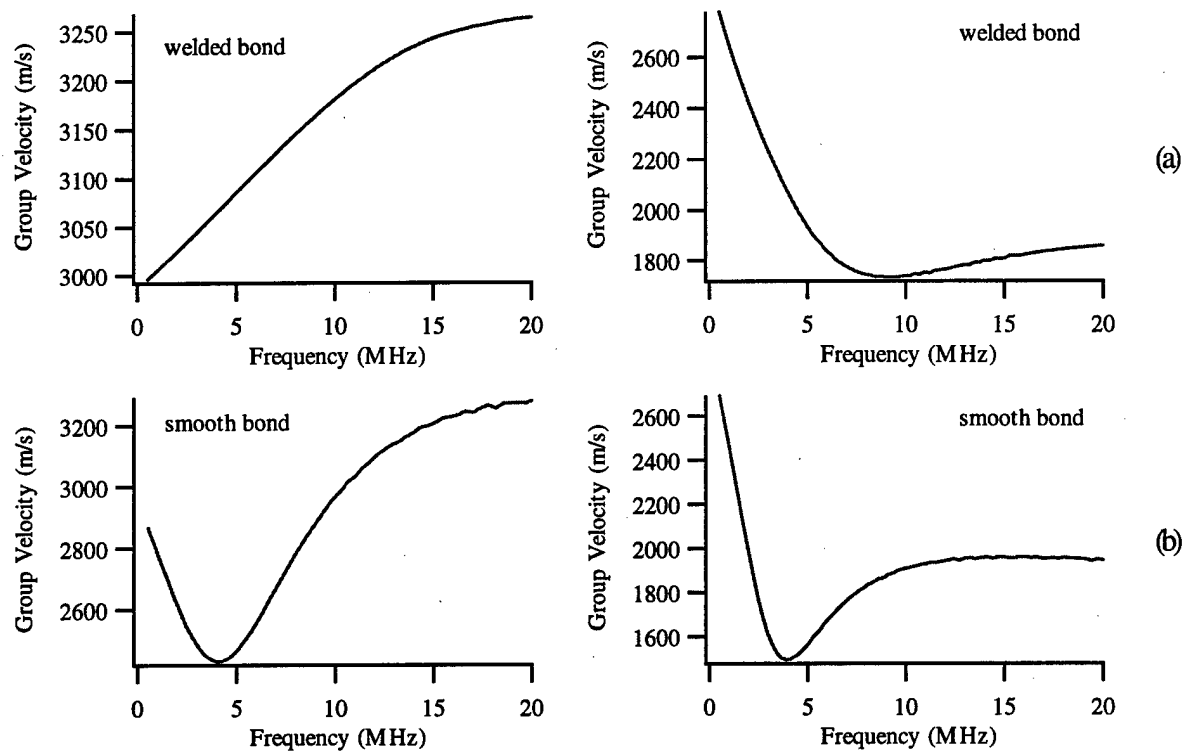


Figure 3. Theoretical dispersion curves calculated from experimental parameters for the coating acoustically stiffer (left) and less stiff than the substrate (right), welded contact (a) and smooth contact (b).

In a subsequent report we will describe in detail the problem with axial symmetry based on the conditions of annular generation. Based on the boundary conditions, welded and smooth, and in the absence of torsion we will further reduce the problem and discuss and compare solutions to those obtained by Achenbach and Epstein (ref 1). We will discuss welded and smooth contact between coating and half space and obtain a distinguishing feature of the bond. Also, simulation results will be discussed.

EXPERIMENT

Samples

Four samples were prepared for the experiment, as seen in Table 1. Two were prepared with a welded bond and the other two with a smooth bond. Tantalum sputtered on ASTM A723 steel and chromium electroplated on ASTM A723 steel were used for the welded bond. To simulate the smooth contact bond, thin sheets of nickel and tantalum were epoxied on copper and ASTM A723 steel substrates, respectively.

Table 1. Experimental Sample Parameters

	Coating Acoustically Less Stiff Than Substrate	Coating Acoustically Stiffer Than Substrate
Welded Contact	Sample	Tantalum on Steel
	Method	Sputtered
	Coating Thickness	0.0035 Inch
Smooth Contact	Sample	Tantalum on Steel
	Method	Epoxied
	Coating Thickness	0.005 Inch

Laser System

The laser ultrasonic system (refs 2,5) consists of a Michelson interferometer, a high-power pulsed laser, and a PC with a high-speed digitizer used to acquire and analyze the data. The high-power laser generates the acoustic waves and the Michelson interferometer detects the ultrasonic signals.

The impulse laser is a Big Sky CFR200 Q-switched Nd:YAG pulsed at 10 Hz. It has a wavelength of 532 nm and produces 70 mJ per each 8 ns pulse. Where the laser contacts the surface of the material, the latter is rapidly heated and cooled; this causes stresses in the material, which are manifested as ultrasound. The impulse laser generates in the shape of a ring approximately 1 inch in diameter and 0.01 inch in width. Only a quarter of the circle is used for generation (3/4 of the circle is blocked with an opaque mask). Both Rayleigh surface waves and bulk ultrasonic waves are generated in a wide range of frequencies.

The nonstabilized Michelson interferometer uses a Melles Griot 05-LHP-991 continuous HeNe with a wavelength of 632.8 nm at 10 mW. A Sonix STR-81G 1 GHz digitizing card located in the PC digitizes the signal from the photodetector. A LabVIEW® program was written to acquire the data from the Sonix digitizing card and average, save, and perform data analysis on the ultrasonic signals.

Data Collection and Analysis

The laser system described above was used to generate and detect surface acoustic waves (ref 2) in these samples. Using the LabVIEW® program, ultrasonic data were digitized at a sampling rate of 1 GHz over a range of 8192 points and were averaged over 200 shots. A phase compensating routine was used to normalize the data because the output of the Michelson interferometer was not phase stabilized.

Wavelet analysis was applied to the Rayleigh surface wave signals to determine the frequency-velocity or dispersion relationship of the experimental signals. A more detailed description of the method used for the wavelet analysis is presented in a related paper (ref 2).

DISCUSSION AND RESULTS

We conducted experiments to generate and analyze Rayleigh surface waves where the layer on half space analysis can apply. In order to investigate a broader range of parameters in the theory, we did measurements for the conditions indicated in Table 1, with the specific coating and substrate materials and type of bonding or deposition given.

The sputtered tantalum-on-steel data show the higher frequencies arriving later and the lower frequencies earlier. This is evident in the dispersion curve obtained from the data by means of the wavelet analysis seen in Figure 4(a). Further, the low-frequency velocity starts at the steel value and drops to the tantalum velocity for higher frequencies. The arrival time of the first Rayleigh signal is between 4.5 and 5 microseconds as in steel, with the displacements due to the tantalum arriving later, illustrating the lower Rayleigh velocity of tantalum. For chromium electrodeposited on steel, the interferometer data show the higher frequency displacements arriving first and before the steel signal. The dispersion curve in Figure 4(b) shows that the velocity at lower frequencies starts at the lower steel value and at the higher frequencies rises to the chromium value. For intermediate frequencies the data show intermittent velocities. The results of theoretical analysis of the dispersion, Figure 3(a), indicate the same features as the ones obtained from experiment and wavelet analysis.

In the smooth contact case, the data are much different than in the welded contact case. In both cases, when the coating is acoustically stiffer than the substrate and less stiff, the ultrasonic signal is much longer in time than in the welded case. The tantalum epoxied-to-steel signal illustrated in Figure 4(c) shows the lower frequencies arriving earlier, but the decreasing frequency trend in the welded tantalum-on-steel case is not seen. The resulting dispersion curve shows, in the lower frequencies, two frequencies traveling at the same velocity below that of the substrate, which is also not seen in the welded case. The chromium-on-steel case that was studied for the welded case, was compared to nickel epoxied to copper for the smooth contact case. Both have a coating that is acoustically stiffer than the substrate. For the latter, the dispersion curve shows two frequencies having the same velocity. As shown from the results of the theoretical dispersion curves, Figure 3(b), both curves exhibit a minimum in the lowest mode. This means that two frequencies have the same velocity. The experimental data for the two smooth contact cases show just such a superposition, with the exception that the dip in the dispersion curves goes to much lower velocities, as seen in Figures 4(c) and (d). Experiments with similar objectives were published by Nagy and Adler (ref 6) and Adler et al. (refs 7,8) for friction-welded specimens. Here the dip in the dispersion curve was related to the pressure and velocity of the spinning member used during joining. Wu et al. (refs 9,10) saw a dip that corresponded to the epoxy bond and the bond thickness. They successfully analyzed their epoxied coating data in terms of three layers.

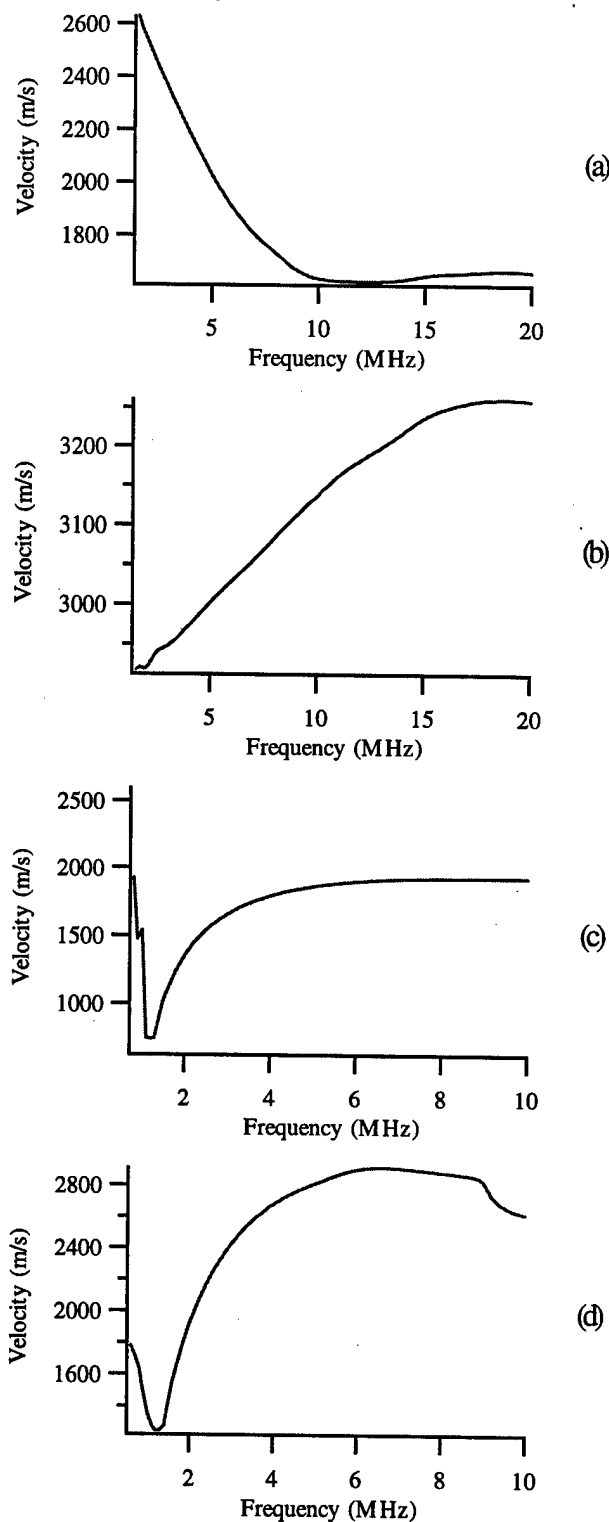
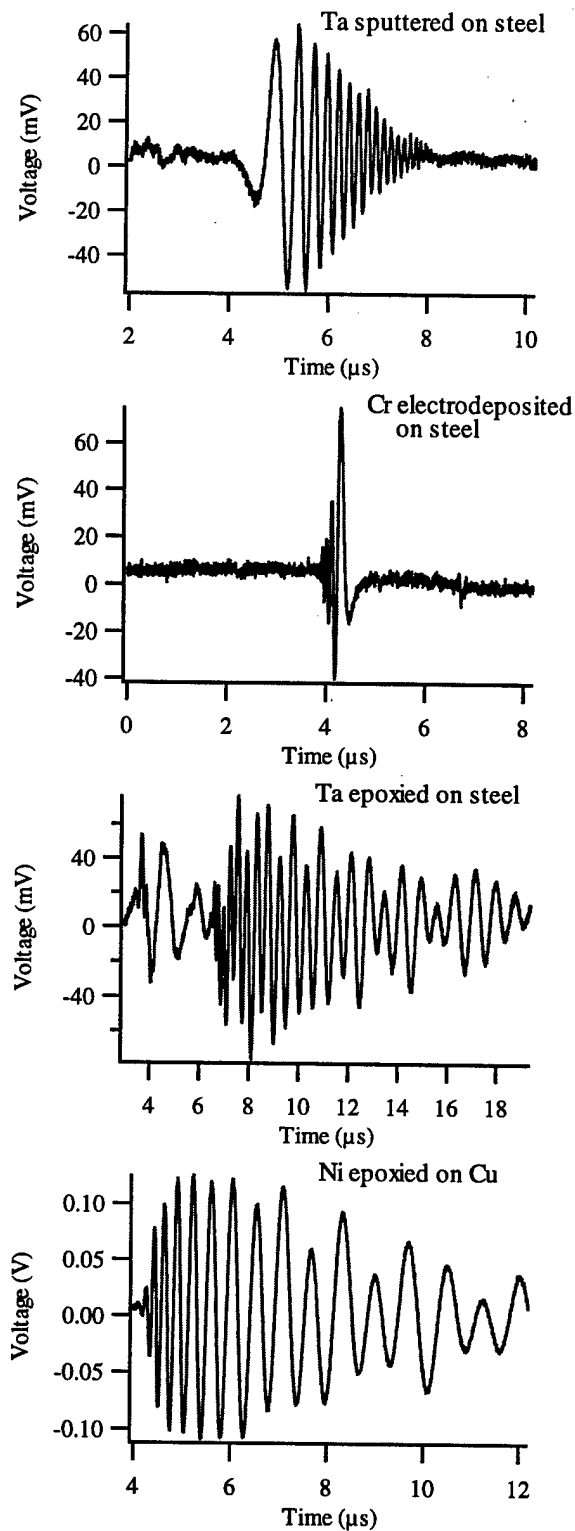


Figure 4. Waveforms from the laser-generated surface waves (left) and their corresponding dispersion curves (right).

CONCLUSIONS

Rayleigh surface waves were generated and detected in coated materials with different bond qualities. Wavelet analysis was used to obtain dispersion curves of these signals. There is a relationship between dispersion of surface waves and coating-substrate bond quality. Theoretical and experimental dispersion curves were obtained for four different cases and compared. The theoretical dispersion curves came from the theory based around Achenbach and Epstein (ref 1). To match our experiment we completed the analysis for annular generation, which did not result in straight-crested waves as in Achenbach and Epstein (ref 1). However, in the absence of torsional deformation, the dispersion curves were identical to those of the straight-crested case.

As indicated in Table 1, we used chromium electrodeposited on steel and tantalum sputtered on steel to achieve the welded bond. The dispersion curves we obtained using wavelets in both cases show the shape one would expect from the analysis, with the high and low frequency values of the Rayleigh velocity corresponding to the coating and substrate, respectively, and a smooth transition between these two values at the intermediate frequencies. As Table 1 also reveals, we epoxied sheets of tantalum and nickel on steel and copper, respectively. We did this to try to approximate the smooth boundary condition between layer and half space. The dispersion curves thus obtained have the approximate shape found from the analysis, but show a more pronounced dip in the low frequency region. The low frequency end of the curves gives the substrate Rayleigh velocity, whereas the higher frequency end gives the velocity for the coating. Even the raw data from the interferometer (after averaging) indicate that a clear differentiation can be made between the welded bond of tantalum sputtered on steel and the approximation of the smooth bond obtained by the tantalum sheet epoxied to steel. The dispersion curves certainly show that difference, as well as the differences in relative stiffness between coating and substrate.

REFERENCES

1. Achenbach, J.D., and Epstein, I., "Dynamic Interaction of a Layer and a Half-Space," *Journal of Engineering Mechanics*, Proceedings of the American Society of Civil Engineers, October 1967, pp. 27-42.
2. Knight, B., Braunstein, J., Cox, J.F., and Frankel, J., "Laser-Ultrasonic Characterization of Electroplated Chromium Coatings," *Review of Progress in QNDE*, Vol. 18A, pp. 365-372.
3. Cielo, P., Nadeau, F., and Lamontagne, M., "Laser Generation of Convergent Acoustic Waves for Materials Inspection," *Ultrasonics*, Vol. 23, No. 2, March 1985, pp. 55-62.
4. Auld, B.A., *Acoustic Fields and Waves in Solids: Vol. 2*, Krieger Publishing Company, Malabar, FL, 1990, p. 108.
5. "LaserWave," Textron Systems Division, 201 Lowell Street, Wilmington, MA 01887-2941.
6. Nagy, P.B., and Adler, L., "Ultrasonic NDE of Solid State Bonds: Inertia and Friction Welds," *Journal of Nondestructive Evaluation*, Vol. 7, No. 3/4, pp.199-215.
7. Adler, L., Billy, M., Quentin, G., Talmant M., and Nagy, P.B., "Generalized Lamb Modes in Friction-Welded Steel Layer on Aluminum," *Review of Progress in QNDE*, Vol. 8B, pp. 1973-1980.
8. Adler, L., Billy, M., Quentin, G., Talmant M., and Nagy, P.B., "Evaluation of Friction-Welded Aluminum-Steel Bonds Using Dispersive Guided Modes of a Layer Substrate," *Journal of Applied Physics*, Vol. 68, No. 12, December 1990, pp. 6072-6076.
9. Wu, T.T., and Chen, Y.Y., "Wavelet Analysis of Laser-Generated Surface Waves in a Layered Structure with Unbond Regions," *Journal of Applied Mechanics*, Vol. 66, June 1999, pp. 507-513.
10. Wu T.T., and Liu, Y.H., "Inverse Determination of Thickness and Elastic Properties of a Bonding Layer Using Laser-Generated Surface Waves," *Ultrasonics*, Vol. 37, 1999, pp. 23-30.

TECHNICAL REPORT INTERNAL DISTRIBUTION LIST

	<u>NO. OF COPIES</u>
TECHNICAL LIBRARY ATTN: AMSTA-AR-CCB-O	5
TECHNICAL PUBLICATIONS & EDITING SECTION ATTN: AMSTA-AR-CCB-O	3
OPERATIONS DIRECTORATE ATTN: SIOWV-ODP-P	1
DIRECTOR, PROCUREMENT & CONTRACTING DIRECTORATE ATTN: SIOWV-PP	1
DIRECTOR, PRODUCT ASSURANCE & TEST DIRECTORATE ATTN: SIOWV-QA	1

NOTE: PLEASE NOTIFY DIRECTOR, BENÉT LABORATORIES, ATTN: AMSTA-AR-CCB-O OF ADDRESS CHANGES.

TECHNICAL REPORT EXTERNAL DISTRIBUTION LIST

<u>NO. OF COPIES</u>	<u>NO. OF COPIES</u>		
DEFENSE TECHNICAL INFO CENTER ATTN: DTIC-OCA (ACQUISITIONS) 8725 JOHN J. KINGMAN ROAD STE 0944 FT. BELVOIR, VA 22060-6218	2	COMMANDER ROCK ISLAND ARSENAL ATTN: SIORI-SEM-L ROCK ISLAND, IL 61299-5001	1
COMMANDER U.S. ARMY ARDEC ATTN: AMSTA-AR-WEE, BLDG. 3022 AMSTA-AR-AET-O, BLDG. 183 AMSTA-AR-FSA, BLDG. 61 AMSTA-AR-FSX AMSTA-AR-FSA-M, BLDG. 61 SO AMSTA-AR-WEL-TL, BLDG. 59	1 1 1 1 1 2	COMMANDER U.S. ARMY TANK-AUTMV R&D COMMAND ATTN: AMSTA-DDL (TECH LIBRARY) WARREN, MI 48397-5000	1
PICATINNY ARSENAL, NJ 07806-5000		COMMANDER U.S. MILITARY ACADEMY ATTN: DEPT OF CIVIL & MECH ENGR WEST POINT, NY 10966-1792	1
DIRECTOR U.S. ARMY RESEARCH LABORATORY ATTN: AMSRL-DD-T, BLDG. 305 ABERDEEN PROVING GROUND, MD 21005-5066	1	U.S. ARMY AVIATION AND MISSILE COM REDSTONE SCIENTIFIC INFO CENTER ATTN: AMSAM-RD-OB-R (DOCUMENTS) REDSTONE ARSENAL, AL 35898-5000	2
DIRECTOR U.S. ARMY RESEARCH LABORATORY ATTN: AMSRL-WM-MB (DR. B. BURNS) ABERDEEN PROVING GROUND, MD 21005-5066	1	COMMANDER U.S. ARMY FOREIGN SCI & TECH CENTER ATTN: DRXST-SD 220 7TH STREET, N.E. CHARLOTTESVILLE, VA 22901	1
COMMANDER U.S. ARMY RESEARCH OFFICE ATTN: TECHNICAL LIBRARIAN P.O. BOX 12211 4300 S. MIAMI BOULEVARD RESEARCH TRIANGLE PARK, NC 27709-2211	1		

NOTE: PLEASE NOTIFY COMMANDER, ARMAMENT RESEARCH, DEVELOPMENT, AND ENGINEERING CENTER,
BENÉT LABORATORIES, CCAC, U.S. ARMY TANK-AUTOMOTIVE AND ARMAMENTS COMMAND,
AMSTA-AR-CCB-O, WATERVLIET, NY 12189-4050 OF ADDRESS CHANGES.
